Soil & Tillage Research 133 (2013) 1–9

Contents lists available at SciVerse ScienceDirect

Soil & Tillage Research

journal homepage: www.elsevier.com/locate/still

Field quantification of wetting–drying cycles to predict temporal changes of soil pore size distribution

G. Bodner *, P. Scholl, H.-P. Kaul

Department of Crop Sciences, Division of Agronomy, University of Natural Resources and Life Sciences, BOKU Vienna, Gregor Mendel Straße 33, A-1190 Vienna, Austria

ARTICLE INFO

Article history:
Received 15 February 2013
Received in revised form 25 April 2013
Accepted 7 May 2013

Keywords:
Wetting–drying cycles
Soil pore size distribution
Spectral analysis
Temporal variability
Tension infiltrometer

ABSTRACT

Wetting–drying (WD) cycles substantially influence structure related soil properties and processes. Most studies on WD effects are based on controlled cycles under laboratory conditions. Our objective was the quantification of WD cycles from field water content measurements and the analysis of their relation to the temporal drift in the soil pore size distribution. Parameters of the Kosugi hydraulic property model ($r_{m,Kosugi}$, σ_{Kosugi}) were derived by inverse optimization from tension infiltrometer measurements. Spectral analysis was used to calculate WD cycle intensity, number and duration from water content time series. WD cycle intensity was the best predictor (r^2 = 0.53–0.57) for the temporal drift in median pore radius ($r_{m,Kosugi}$) and pore radius standard deviation (σ_{Kosugi}). At lower soil moisture conditions the effect of cycle intensity was reduced. A bivariate regression model was derived with WD intensity and a meteorological indicator for drying periods (ET_0, climatic water balance deficit) as predictor variables. This model showed that WD enhanced macroporosity (higher $r_{m,Kosugi}$) while decreasing pore heterogeneity (lower σ_{Kosugi}). A drying period with high cumulative values of ET_0 or a strong climatic water balance deficit on the contrary reduced $r_{m,Kosugi}$ while slightly increasing σ_{Kosugi} due to higher frequency at small pore radius classes. The two parameter regression model was applied to predict the time course of soil pore size distribution parameters. The observed system dynamics was captured substantially better by the calculated values compared to a static representation with averaged hydraulic parameters. The study showed that spectral analysis is an adequate approach for the quantification of field WD pattern and that WD intensity is a key factor for the temporal dynamics of the soil pore size distribution.

1. Introduction

Hydraulic properties of the soil depend on texture and structure. In the saturated and near-saturated range soil structure essentially controls the two fundamental relations for water flow, i.e. the retention and hydraulic conductivity functions (Cresswell et al., 1992). Soil structural porosity is a highly dynamic property that responds to various external factors of environmental and human nature. Therefore knowledge of spatial and temporal variability of soil hydraulic properties is fundamental to accurately describe processes like water infiltration and storage (van Es et al., 1999).

In a tillage experiment, Schwen et al. (2011) showed that seasonal variability of hydraulic properties was higher than tillage induced variability. Bodner et al. (2008) studied the effect of different cover crop canopy and residue coverage on hydraulic properties and found significant over winter decrease in hydraulic conductivity and flow weighted pore radius for all treatments. The effect was more pronounced in bare soil. Also, irrigation can introduce strong temporal changes of hydraulic properties depending on soil type and irrigation method (Angulo-Jaramillo et al., 1997; Zeng et al., 2013).

The role of environmental influences on soil structure formation was reviewed by Horn and Smucker (2005). In arid, semi-arid and subhumid regions wetting–drying (WD) cycles are essential for soil aggregation (Dalal and Bridge, 1996). Intensity, number and duration of swelling and shrinkage cycles were identified as key processes of aggregate formation and strength. Capillarity was the driving factor of soil aggregation upon drying, while rewetting increased structural instability (Peng et al., 2007; Lado et al., 2004).

Abbreviations: WD, wetting–drying; PSD, pore size distribution; ϕ, total porosity; θ_s, water content at saturation; θ_r, residual water content; $h_{m,Kosugi}$, median pressure head; $r_{m,Kosugi}$, median pore radius; σ_{Kosugi}, pore radius standard deviation.

* Corresponding author. Tel.: +43 1 47654 3331; fax: +43 1 47654 3342.
E-mail address: gernot.bodner@boku.ac.at (G. Bodner).

0167-1987© 2013 The Authors. Published by Elsevier B.V. Open access under CC BY-NC-ND license.
http://dx.doi.org/10.1016/j.still.2013.05.006

Soil porosity was found to increase after the application of WD cycles (Pires et al., 2005). Pires et al. (2009) observed an evolution from massive structures to structures with a great number of large and connected pores after WD cycles. Also the pore size distribution (PSD) is modified in response to internal capillary stresses. Sartori et al. (1985) and Pagliai et al. (1987) discussed the overall influence of WD cycles on total porosity, pore shape and pore size distribution. Their results demonstrate an increase in the volume of pores in the range of 30 μm to 1 mm and strong modifications in shape and size distribution.

An increase in coarse pores during drying was described as a consequence of crack and microcrack formation (Bruand and Prost, 1987; Horn et al., 2002; Seguel and Horn, 2006). Pires et al. (2005) also found an increase in the number of micropores and mesopores with subsequent WD cycles. Sarmah et al. (1996) however observed a decrease in water infiltration rate after WD cycles. This was probably due to the slaking and collapse of aggregates. Also Phogat and Aylmore (1989) found a decrease in macroporosity after cycles of soil wetting and subsequent drying. Macropores are generally more sensitive to soil deformation than micropores because of lower pore rigidity (Kutílek et al., 2006). However, Braudeau et al. (2004) suggested that shrinkage capacity of macropores can also be less than that of micropores due to smaller capillary stresses in large pores.

Peng et al. (2007) conducted a detailed laboratory study on pore changes under varying WD cycle intensity and number. Intense WD cycles enhanced the volume of large pores markedly in most soils they analyzed. Their data also suggested higher pore heterogeneity with increasing cycle number. However, if soils were subjected to intense WD cycles, the frequency dependent effect faded. Several authors showed that the impact of the first WD cycle on soil structure is greatest and decreases with subsequent cycles (Basma et al., 1996; Tripathy et al., 2002; Leij et al., 2002). The effect however also depends on the initial state of soil (pre-shrinkage stress; Baumgartl and Horn, 1999).

Most quantitative knowledge on WD effects on soil properties has been obtained from laboratory experiment with soil samples subject to controlled cycles. But also in field experiments several authors referred to WD as major influence on hydraulic property and soil structure changes (e.g. Mapa et al., 1986; Pagliai et al., 2004; Mubarak et al., 2009). A main gap in our current knowledge is to understand how irregular cycles typically occurring under field conditions modify hydraulic properties. A quantification of the natural WD pattern in field experiments would be highly necessary in order to better understand their role as a driver for hydraulic property and soil structure dynamics in a natural soil environment. This could help to bridge process based understanding from laboratory work and qualitative field observations.

The objective of our study therefore was to develop a method to quantify the WD pattern from field soil water content time series using spectral analysis. We then analyzed the relation between WD and temporal changes of Kosugi's retention curve parameters that capture the shape of the pore size distribution. Finally our aim was to test a regression model to predict the time course of Kosugi's pore parameters from environmental variables.

2. Materials and methods

2.1. Field experiment

A field experiment was conducted over three years (2009–2012) to study factors underlying temporal changes in soil hydraulic properties. The experiment is described in detail by Bodner et al. (2013). In short, it was located on an arable field near Raasdorf, Lower Austria (48°14′ N, 16°35′ E, 156 m asl). The main experimental factor was three different post-harvest soil cover treatments. For the present evaluation, we averaged data from all plots (n = 9) as our focus was on the mean temporal dynamics at the site. Climatically the location is characterized by sub-humid conditions (pannonic) with an average annual precipitation of 525 mm, a mean annual temperature of 9.8 °C, and a mean relative humidity of 75%. Weather data were recorded by an automated weather station (Adcon Telemetry GmbH, Austria) directly on the field. Fig. 1 shows rainfall, temperature and reference evapotranspiration (ET_0) for the three experimental years.

The soil is classified as Chernozem in the WRB (IUSS, 2007). Basic soil properties are given in Table 1.

Soil water content was monitored continuously in each plot by capacitance sensors (CProbe, Adcon Telemetry GmbH, Austria) installed via access tubes. Sensors were previously normalized and compared to gravimetric reference samples. Fig. 2 shows the soil water dynamics in the upper soil layer (5 cm soil depth) which was used for the analysis of WD cycles.

2.2. Determination of soil pore size distribution parameters

Soil pore size distribution parameters were determined by inverse analysis of tension infiltrometer data. Infiltration measurements were conducted twelve times between September 2009 and July 2012. All measurements were performed using a tension infiltrometer (Soil Measurement Systems Inc., Tucson, AZ) and taken at the soil surface where most structural dynamics were expected. Details of measurement are given in Bodner et al. (2013).

The inverse analysis of infiltration measurements requires a numerical solution of the Richards equation for Darcian flow in a radial symmetric 2D domain. We followed the procedure presented by Šimůnek et al. (1998). Soil water retention was described by the model of Kosugi (1996) which is based on a lognormal pore size distribution. Soil water retention Se(h) is given by

$$\mathrm{Se}(h) = 0.5 Erfc\left(\frac{\log(h/(h_{\mathrm{m,Kosugi}}))}{\sqrt{2}\sigma_{\mathrm{Kosugi}}}\right) \quad (1)$$

where Se is the effective saturation corresponding to $(\theta - \theta_r)/(\theta_s - \theta_r)$ with θ (cm^3 cm^{-3}) being volumetric water content, θ_r (cm^3 cm^{-3}) residual water content and θ_s (cm^3 cm^{-3}) saturation water content. *Erfc* is the complementary error function, $h_{\mathrm{m,Kosugi}}$ (cm) the median pressure head of the soil water retention curve where Se($h_{\mathrm{m,Kosugi}}$) = 0.5, and σ_{Kosugi} the standard deviation of the log-transformed pressure head. The median pore radius ($r_{\mathrm{m,Kosugi}}$) can be calculated from $h_{\mathrm{m,Kosugi}}$ using the Young–Laplace equation.

Parameter estimation is done by minimizing the objective function as defined by Šimůnek and van Genuchten (1996) using the program HYDRUS 2D/3D (Šimůnek et al., 2006) which applies a Levenberg–Marquardt nonlinear minimization algorithm. Initial parameter estimates were derived from the texture based

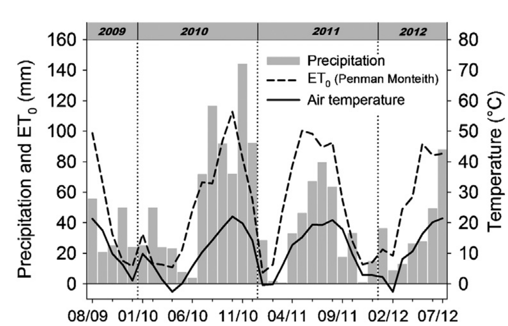

Fig. 1. Monthly averaged precipitation, air temperature and reference evapotranspiration (ET_0) at the experimental site.

Table 1
Soil properties of the experimental field.

Horizon	Depth (cm)	Sand ($kg\,kg^{-1}$)	Silt ($kg\,kg^{-1}$)	Clay ($kg\,kg^{-1}$)	Texture USDA	C_{org} ($kg\,kg^{-1}$)	Field capacity ($cm^3\,cm^{-3}$)	Wilting point ($cm^3\,cm^{-3}$)
A	0–40	0.19	0.57	0.24	SiL	0.025	0.32	0.15
AC	40–55	0.23	0.54	0.23	SiL	0.015	0.27	0.10
C	>55	0.22	0.62	0.16	SiL	0.008	0.25	0.07

pedotransfer function Rosetta (Schaap et al., 2001) (input parameters: soil texture and bulk density). To reduce the amount of unknown variables, θ_r was fixed to 0.067 $cm^3\,cm^{-3}$, as predicted by Rosetta. θ_s values were set equal total porosity from sample cylinder measurements, and K_s was used from direct Wooding analysis of infiltration data (Šimůnek et al., 1998; Bodner et al., 2013). The remaining parameters σ_{Kosugi}, and $h_{m,Kosugi}$ were then estimated inversely.

2.3. Quantification of wetting–drying cycles

WD cycles were quantified by spectral analysis of surface near soil water content time series (5 cm soil depth) using the SAS procedure PROC SPECTRA (SAS/STAT, 2009). Spectral analysis is a statistical method that can discern cyclic patterns in a soil property (Nielsen and Wendroth, 2003; Si, 2008). We quantified the intensity of WD cycles by spectral density and calculated the number of cycles from spectral wavelength (cycle duration) via

$$N_{cycles} = \frac{p_i}{\Delta t_{i,i+i}} \tag{2}$$

where N_{cycles} is the number of wetting–drying cycles, p_i (days) is the wavelength of a spectral peak and $\Delta t_{i,i+1}$ (days) is the length of the analyzed time series. Fig. 3 exemplifies our approach to quantification of WD cycles.

Before applying spectral analysis data are detrended by linear regression of water content vs. time (Worrall and Burt, 1998, Fig. 3a). For each period it is tested if the detected spectra are different from random scattering (white noise) by a Fisher's Kappa and Bartlett's Kolmogorov–Smirnov statistics which are available in the SAS spectral procedure.

Spectral analysis then produces estimates of spectral densities by a finite Fourier transform which decomposes the data series into a sum of sine and cosine waves of different amplitudes and wavelengths (Eq. (3)):

$$x_t = \frac{a_0}{2} + \sum_{k=1}^{m} [a_k \cos(\omega_k t) + b_k \sin(\omega_k t)] \tag{3}$$

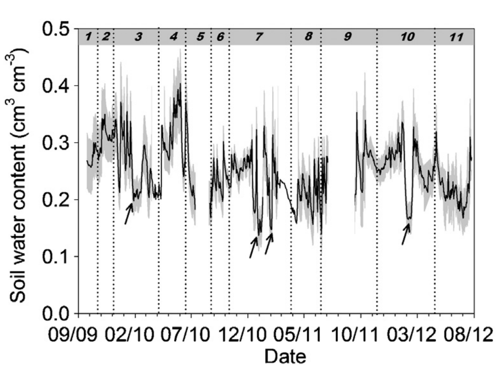

Fig. 2. Soil water content in the surface near soil layer (5 cm soil depth). Gray area shows the standard deviation ($n = 9$), vertical dotted lines indicate measurement dates and numbers define periods between infiltration measurements. Arrows show periods of frozen soil. Gaps are due to sensor removal during harvest and seeding operations.

Here x_t is the value of a time series at time t, m is the number of frequencies in the Fourier decomposition ($m = n/2$ if n is even, $m = n - 1/2$ if n is odd, where n is the number of observations in the time series), a_0 is the mean term ($2\bar{x}$), a_k and b_k are the cosine and sine coefficients respectively and ω_k are the Fourier frequencies ($\omega_k = 2\pi k/n$). The periodogram of amplitude at each frequency k is given by

$$J_k = \frac{n}{2}(a_k^2 + b_k^2) \tag{4}$$

Fig. 3b gives an example of a periodogram with spectral densities for the detrended series. The white noise spectrum as well as the 95% confidence limit for peaks significantly differing from white noise are calculated following Torrence and Compo (1998). The periodogram can be interpreted as contribution of the kth harmonic ω_k to the total sum of squares in the decomposition of the process. Thus a high spectral density quantifies a strong cyclic deviation from the mean of the time series. Fig. 3c shows the wave function of the dominant spectrum for the example series, i.e. the sum of cosine and sine components weighted by a_k and b_k at frequency 0.161 over time. When summing up all significant spectra according to Eq. (4) the reconstructed time series shown in Fig. 3d is obtained. To reduce volatility of the periodogram, generally spectra are smoothed using e.g. a moving average to obtain the final spectral density estimates (SAS/STAT, 2009). We applied a third order moving average for smoothing the periodograms.

2.4. Statistical analyses and modeling

Statistical analyses of the data comprised (i) analysis of variance of soil pore size distribution parameters, (ii) regression analysis of the relation between pore parameters and WD pattern, and (iii) evaluation of a regression based predictive model for the time course of soil pore size distribution parameters.

2.4.1. Analysis of variance

Soil hydraulic parameters (σ_{Kosugi} and $r_{m,Kosugi}$) were submitted to an analysis of variance to determine periods of significant temporal drift. We used the MIXED procedure in SAS to properly consider repeated measurements over time. PROC MIXED computes Wald-type F-statistics using generalized least squares (GLSE) based on restricted maximum likelihood estimates of the variance components (Littell et al., 1998). In case of significant differences in the Wald-F-statistic for $p < 0.05$, treatment means were compared using a two-sided t test. To account for the serial correlation of non-randomized repeated measures on the same experimental unit, i.e. measurement date, an adequate correlation model was fit to the data based on the Akaike Information Criterion (Piepho et al., 2004).

2.4.2. Regression model

Regression analysis was used to determine the relation between temporal drift in soil pore size distribution parameters and WD characteristics. The objective was to obtain a predictive model for hydraulic parameter change over time driven by independent environmental variables. The SAS procedure PROC REG with the RSQUARE selection method was used to find subsets

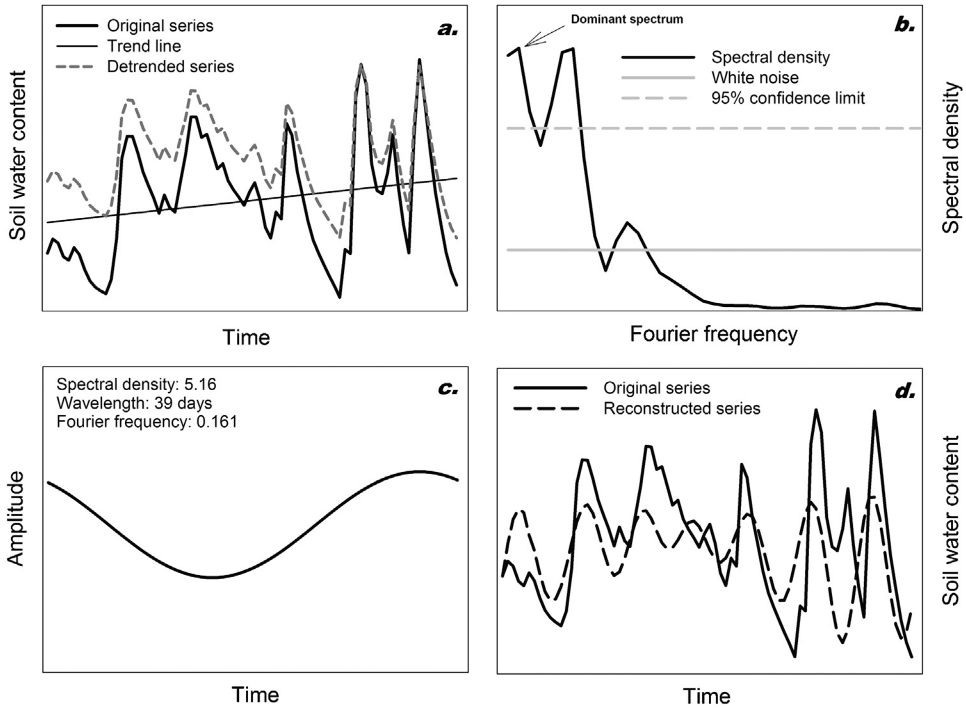

Fig. 3. Spectral analysis of water content time series. (a) Detrending of the initial series, (b) spectral density periodogram of the series with white noise spectrum and 95% confidence limits, (c) wave function of the dominant spectrum, and (d) reconstructed time series from all significant spectra.

of independent variables that best predicted the hydraulic parameters. We restricted to univariate and bivariate models in order to avoid over-parameterization and ensure model interpretability.

Beside WD indicators (cycle intensity, number and duration), some other environmental variables were included. A longer time interval is likely to show higher temporal change. Thus the influence of the length of time separating two measurements ($\Delta t_{i,i+1}$) was tested. The initial value at t_i can also influence the subsequent drift as certain hydraulic property configurations (e.g. a state with more macropores) might be less stable and therefore undergo higher change. The relation between initial value and subsequent drift was therefore analyzed. Also higher soil moisture could increase structural instability resulting in higher temporal drift. This was tested by the influence of initial and average moisture. Beside a cyclic WD pattern, also a general trend of wetting or drying can influences hydraulic properties. Moisture trend, calculated as the slope of a linear regression through water content vs. time between, and meteorological indicators of wetting vs. drying periods (cumulative values of ET_0, rainfall and climatic water balance deficit) were included. The climatic water balance deficit was calculated as the cumulative sum of rainfall minus ET_0 over time.

2.4.3. Model application and evaluation

The regression model obtained from the above analysis was then used to predict the temporal dynamics of pore size distribution parameters at a weekly time step. An initial soil water content series of three weeks was used to ensure a sufficient length of the time series for spectral analysis. Thereafter the series was increased stepwise with the subsequent seven days of water content measurements. A main question was at which value the thresholds for driving variables should be set that determine when hydraulic parameters are updated. We calibrated these thresholds based on the values which separated periods of statistically significant vs. non-significant drift in measured pore parameters. Comparing measured and predicted parameters using varying thresholds revealed that mean values at the periods of significant change in measured hydraulic parameters were the most appropriate tresholds. Whenever these thresholds were achieved, soil hydraulic parameters were updated by the regression model. Afterwards analysis restarted with the subsequent three weeks data as initial time series.

The functional form of the temporal drift between two data points cannot be answered from our data. We applied a cubic hermite spline interpolation between data points using the MATLAB *pchip*-function to obtain a continuous time course of pore parameters.

The model was evaluated with different goodness of fit indices. Root mean squared error (RMSE) is a dimensional squared statistic for difference between measured and modeled values. Modeling efficiency (EF) and the index of agreement (d) are both extensions of the common r^2 statistics of regression lines. EF can get either positive or negative values, 1 being the upper limit, while negative infinity is the theoretical lower bound. EF values lower than 0 result from a worse fit than the average of measurements. The values of the index of agreement lie between 0 and 1, with 1 being the upper limit. Finally the slope and r^2 between modeled and measured values is indicated. All indices were calculated using the IRENE software (Fila et al., 2003).

3. Results and discussion

3.1. Temporal variability of soil pore size distribution parameters

Table 2 gives a summary of the parameters of Kosugi's retention model obtained by inverse parameter optimization from tension infiltrometer measurements. We focus on the parameters describing the shape of the pore size distribution ($r_{m,Kosugi}$, σ_{Kosugi}). A companion paper of Bodner et al. (2013) also demonstrated that θ_s showed only minor temporal changes at site. Therefore we just considered the shape parameters of Kosugi's retention model.

Table 2
Results of analysis of variance for soil hydraulic parameters.

	$r_{m,Kosugi}$ (mm)	σ_{Kosugi}
Statistics summary		
Mean	0.077	1.98
SD	0.078	0.58
CV %	100.8	29.1
Level of significance		
Coverage (C)	NS	*
Time (T)	***	***
Replicate (R)	NS	NS
C × T	NS	NS
R × T	NS	NS

NS is non significant.
* Significant at $p < 0.05$.
*** Significant at $p < 0.001$.

Šimůnek et al. (1998) demonstrated that in the dry range retention curves from inverse estimation deviated from laboratory measurements with a pressure plate extractor. They showed that the inversely estimated curves could better reproduce a field measured infiltration process in a forward simulation. Therefore we consider the inverse estimates from field data appropriate to describe hydraulic properties, particularly for the structural range which we are studying here.

Hayashi et al. (2006) demonstrated that Kosugi's pore parameters are proper indicators for structural porosity. A high $r_{m,Kosugi}$ for a given soil texture class reveals the importance of macroporosity. A narrow pore size distribution (low σ_{Kosugi}) with a high frequency of the dominant pore radius class is characteristic for less structured soils. Šimůnek (2006) gives Kosugi parameters for a range of texture classes. The average values we obtained by parameter optimization ($h_{m,Kosugi}$ 126.5 cm, σ_{Kosugi} 1.98) were between those of sandy loams ($h_{m,Kosugi}$ 27.4 cm, σ_{Kosugi} 1.26) and silty loams ($h_{m,Kosugi}$ 325.9 cm, σ_{Kosugi} 2.30) indicated by Šimůnek (2006). We notice that the average $h_{m,Kosugi}$ (126.5 cm) has to be calculated directly from the optimization results as for mathematical reasons $((1/n)\sum(1/x) \neq 1/(1/n\sum x))$ it cannot be recalculated from the average $r_{m,Kosugi}$ given in Table 2. The coefficient of variation was higher for $r_{m,Kosugi}$ compared to σ_{Kosugi}. The temporal factor was the dominant contribution to the overall variance and was significant for both hydraulic parameters. In average σ_{Kosugi} also differed among soil cover treatments. However there was no interaction of the treatment main effect with time. Therefore the use of mean values at each measurement point provided a good representation of the soil specific parameter range and the temporal dynamics at the site (Fig. 4).

From Fig. 4 a tendency of overwinter increase of $r_{m,Kosugi}$ and a concomitant decrease in σ_{Kosugi} can be observed. Over-winter freezing–thawing has been described to induce aggregate breakdown (Oztas and Fayetorbay, 2003) which would explain structure homogenization as expressed by the reduction of σ_{Kosugi}. Unger (1991) described soil loosening over winter leading to higher aggregate mean weight diameter and reduced bulk density. These processes could result in higher macroporosity as observed in our measurements. During the summer month a decreasing trend in $r_{m,Kosugi}$ and an increase in σ_{Kosugi} could be observed. This might be related to capillary induced soil shrinkage reducing the median radius of pores while pore heterogeneity increased by formation of microfissures (Leij et al., 2002). During the rest of the season, periods of increase as well as decrease in hydraulic parameters were found with a particularly pronounced change between spring and early summer 2010.

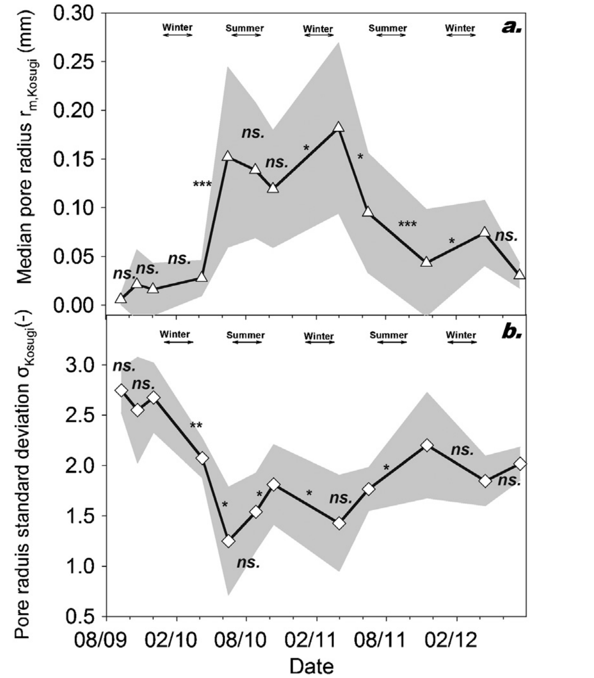

Fig. 4. Temporal variability of the parameters from Kosugi's (1996) water retention model. Statistical comparison indicates if changes between two consecutive measurement dates are significant at $p < 0.05$ (^{ns}non significant, *significant at $p < 0.05$, **significant at $p < 0.01$, ***significant at $p < 0.001$).

3.2. Wetting–drying dynamics

Laboratory experiments demonstrated the dominant influence of WD cycles on hydraulic properties (e.g. Peng et al., 2007). Also field studies with simulated rainfall and subsequent drying (Mubarak et al., 2009) reported strong effects of WD. Under natural conditions the cyclic pattern is more complex and irregular compared to induced WD. This is challenging when studying the impact on field soil properties. We applied spectral analysis of water content time series to quantify cycle intensity, number and duration from spectral density and wavelength. Fig. 5 gives the spectral density periodograms showing the cyclic pattern during each period between hydraulic property measurements.

All periods had cycles with spectra significantly different from white noise. Fig. 5 clearly shows that the value of spectral density expressed the strength of temporal fluctuations of water content (cf. period 1 vs. period 9). Periods with both low and high frequency water content fluctuations resulted in bimodal to multimodal spectral periodograms (cf. periods 7 and 8), although the secondary spectral peaks were frequently below the 95% confidence limit (cf. period 7).

Period one to five as well as period 11 had a dominant spectral peak at the lowest Fourier frequency, indicating that there was one dominant WD cycle. Period one had the lowest cycle intensity which is obvious regarding the low water content fluctuations. Period three to five and period 11 on the contrary had all high spectral peaks indicating an intense WD cycle.

Period six to ten showed dominant spectra at higher frequency, representing cycles of shorter duration with repeated WD over time. For example period eight had a marked bimodal periodogram corresponding to two (first peak) and seven (second peak) cycles of similar intensity that occurred during this period.

The strongest cycle intensities were found between April and June 2010 and between November 2011 and April 2012. These periods were characterized by frequent rainfall events which

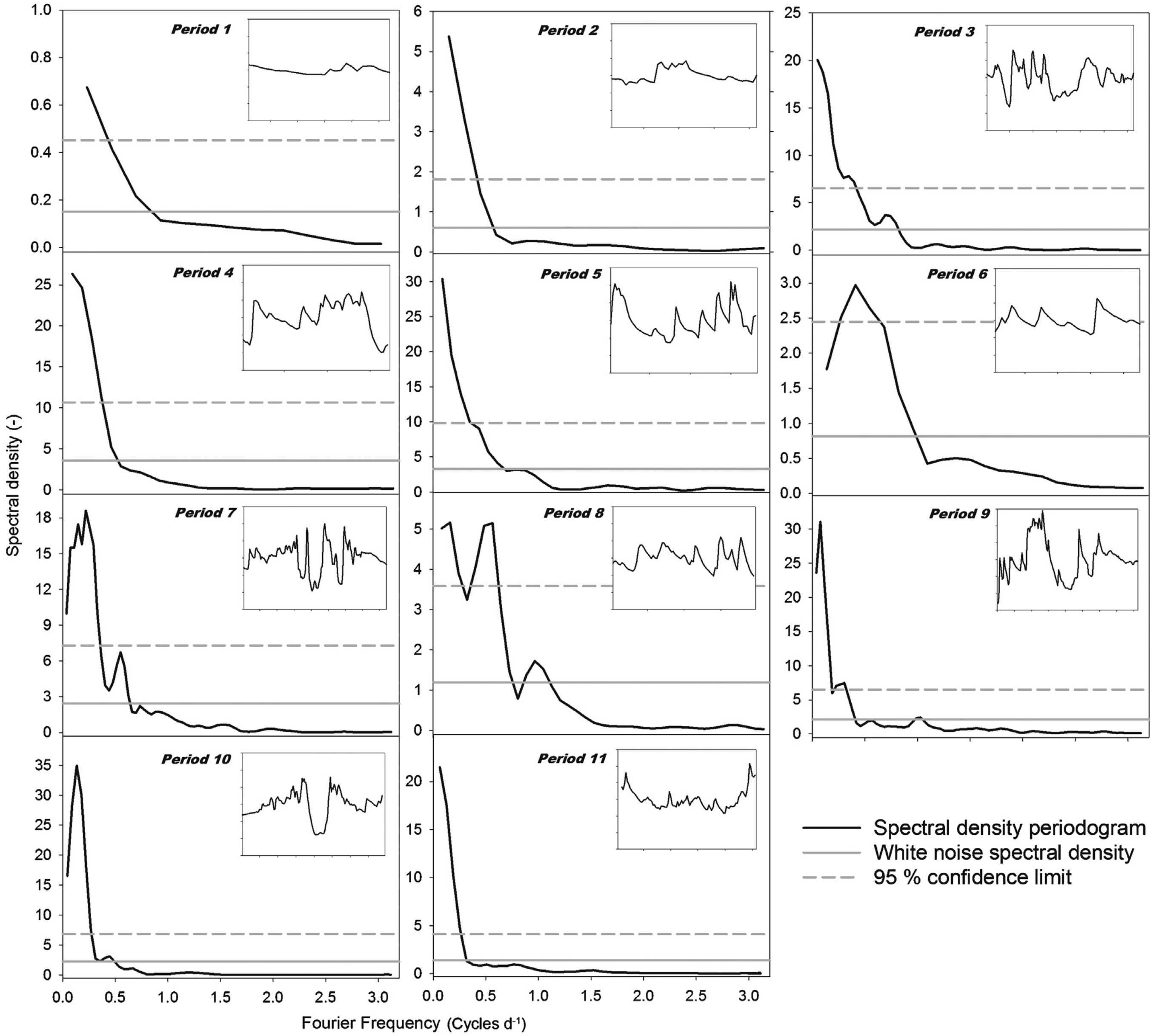

Fig. 5. Spectral density periodograms of WD cycles for the periods between hydraulic property measurements. The underlying detrended water content series is shown in the right corner of each periodogram.

partially explained the intensity of the WD pattern ($r^2 = 0.51$, $p = 0.01$). During October 2010 to June 2011 there were periods with a high number of cycles (high frequency fluctuations). This season was substantially drier than the long-term average (176.6 mm vs. 360.5 mm). However there was no meteorological variable other than the number of rain events, which had only an intermediate r^2, to reliably predict the cyclic behavior of soil WD. Spectral analysis thus provides a unique driving parameter for the analysis of soil processes and properties under field conditions.

3.3. Wetting–drying induced change in soil pore size distribution

In a recent study of Bodner et al. (2013) on the same experiment, they demonstrated that within-season variability of the pore size distribution was strongly related to WD, while over-season dynamics were mainly influenced by soil mechanical disturbance and crop rotation.

Following quantification of the WD pattern, we therefore analyzed its predictive power for temporal changes in Kosugi's PSD parameters. Beside WD, also the influence of (i) initial values of the respective hydraulic variable, (ii) different length of periods between two measurements, and (iii) other moisture related parameters (moisture trend, average moisture, initial moisture, cumulative rain, ET_0, climatic water balance deficit) was tested. Table 3 shows the results of regression analysis. For the bivariate case, only the best model for each parameter is reported.

WD was the best single predictor variable for the temporal drift in both hydraulic parameters. Changes in $r_{m,\text{Kosugi}}$ were also significantly influenced by the climatic water balance deficit. Although there was no direct effect of average soil moisture on WD cycle intensity ($r^2 = 0.04$), it can still modify its impact on soil properties (Watts et al., 1996). We therefore introduced the average soil moisture as a weighting factor. The consistent increase in r^2 confirmed the assumption that WD effects on pore parameters are strongly mediated by the prevailing moisture conditions, with

Table 3
Regression models to predict changes in soil hydraulic property parameters. (Bold values indicate models with all predictor variables being significant.).

	$r_{m,\mathrm{Kosugi}}$	σ_{Kosugi}
Initial value	0.20	0.10
Period length	0.03	0.04
Cycle intensity	**0.43**	**0.50**
Cycle number	<0.01	<0.01
Cycle duration	0.04	<0.01
Cycle intensity$_{\mathrm{weighted}}$	**0.53**	**0.57**
Average moisture	0.33	0.22
Initial moisture	0.01	0.08
Sum rain	>0.01	0.04
Sum ET_0	0.18	0.18
Rain-ET_0	**0.43**	0.10
Intensity$_{\mathrm{weighted}}$ + rain-ET_0	**0.81**	**0.50**
Intensity$_{\mathrm{weighted}}$ + sum ET_0	**0.74**	**0.78**

decreasing impact under low moisture conditions. We also tested other weighting factors for WD intensity such as cycle number and cycle duration. The underlying assumption was that more frequent or longer cycles had a stronger impact. However this did not improve the predictive power of cycle intensity alone. It confirms the dominant influence of cycle intensity on pore size distribution parameters, while cycle number and duration being of subordinated importance (Peng et al., 2007).

As expected bivariate regression models achieved a higher r^2 (cf. Table 3). The intercept in the bivariate models was non-significant, while both predictor variables were significant. Therefore we used zero-intercept models. Beside the higher r^2, the bivariate models also allow a better interpretation of the distinct variables driving increase vs. decrease in hydraulic parameters. Fig. 6 shows the regression models with highest r^2 for the temporal drift in the Kosugi parameters.

The change in PSD predicted by the regression models is resumed in Fig. 7. Intense WD cycles increased the median pore radius (+8.0% per unit cycle intensity), while the pore radius

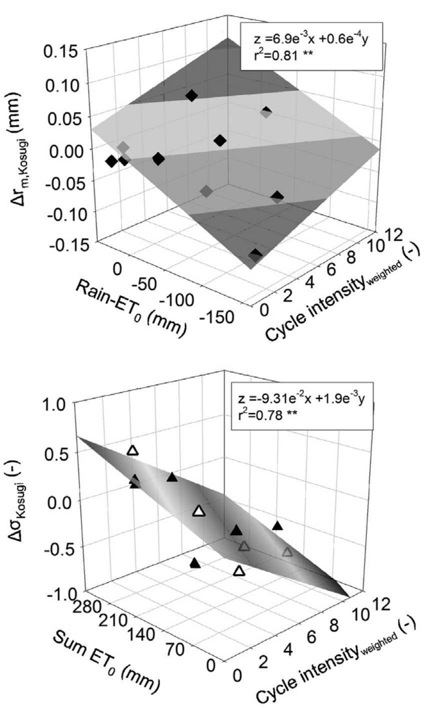

Fig. 6. Bivariate regression models between environmental driving forces and the temporal drift in the parameters of Kosugi's hydraulic property model.

standard deviation decreased (−3.5% per unit cycle intensity). A prolonged dry period (indicated by a high ET_0 and a high climatic water balance deficit respectively) led to a reduction of the median pore radius (−3.0% per −10 mm decrease in the water balance deficit), while slightly increasing pore radius standard deviation (+1% per 10 mm increase in cumulative ET_0) with a higher frequency of fine pores.

Also Peng et al. (2007) reported a general increase in porosity (between 2.6 and 16.5% depending on clay content) with WD cycle intensity and highest changes in the macropore fraction. On the other hand Leij et al. (2002) showed that drying reduced structural porosity due to aggregate coalescence. They also reported an increase in fine pore frequency. Our model suggests that the cyclic pattern of WD drives the formation of structural (macro)porosity, while capillary driven aggregate coalescence is the predominant process during a general drying phase increasing the amount of smaller pore classes at the expense of macropores.

We want to point out that the effect of WD is expected to strongly interact with other drivers of changes in structural porosity such as tillage. A loose soil after tillage will show different response to repeated WD compared to a more stable no-till soil (e.g. Pagliai et al., 2004). Also different soil textures will respond differently to WD as shown by Peng et al. (2007).

3.4. Prediction of pore size distribution parameters

The regression models were used to predict the time course of Kosugi's pore parameters. WD was calculated from water content data by spectral analysis with a weekly time step. ET_0 and cumulative water balance were obtained from meteorological data. The threshold value for the moisture weighted cycle intensity was set to six for both $\Delta\sigma_{\mathrm{Kosugi}}$ and $\Delta r_{m,\mathrm{Kosugi}}$. Periods of non-significant change in Kosugi parameters had an average weighted cycle intensity of 3.8, while those periods showing significant changes had an intensity of 6.3. Thus six seemed a reasonable intensity threshold to update the hydraulic parameters based on the regression model. Thresholds for cumulative ET_0 were set at 100 mm ($\Delta\sigma_{\mathrm{Kosugi}}$) and for climatic water balance deficit at −50 mm ($\Delta r_{m,\mathrm{Kosugi}}$). Fig. 8 shows the predicted temporal dynamics of the hydraulic parameters compared to the range of measured data.

Generally the hydraulic property dynamics were reproduced satisfactorily by the model with a slight tendency to underestimate the measured values. A major deviation between the modeled time course and observed values occurred during autumn 2011 (measurement point in November 2011) where the model did not capture the decrease in $r_{m,\mathrm{Kosugi}}$ and the increase in σ_{Kosugi}. The autumn season 2011 was particularly dry (47.8 mm vs. 107.8 mm long-term average rainfall). It is likely that the ET_0-based meteorological variables in our model did not sufficiently reflect soil surface drying and concomitant hydraulic parameter drift in this period.

The deviation between the measurement point in December 2009 and the modeled time course is mainly related to the problem of interpolation. The model predicated the first update in hydraulic parameters for the 3rd February 2010 with WD cycle higher than the set threshold. When linking the initial values with the calculated data points at this date by a cubic spline however, it was not possible to capture the prolonged period of unchanged pore parameters in the beginning. As mentioned above, our model is not able to predict the exact functional behavior between two data points.

Table 4 gives the goodness of fit indices between measured and calculated hydraulic parameters.

In hydrological modeling generally static hydraulic parameters are used. The indices however showed clearly that the calculated

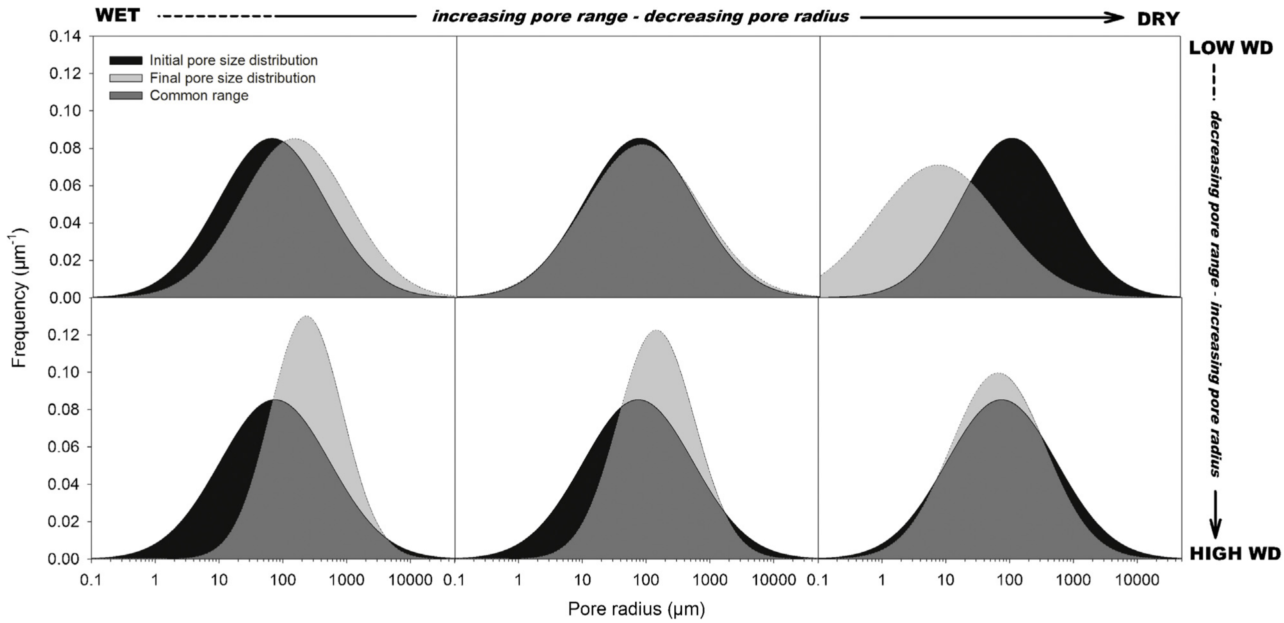

Fig. 7. Dynamics of the pore size distribution driven by wetting and drying indicators as predicted by the regression models in Fig. 6.

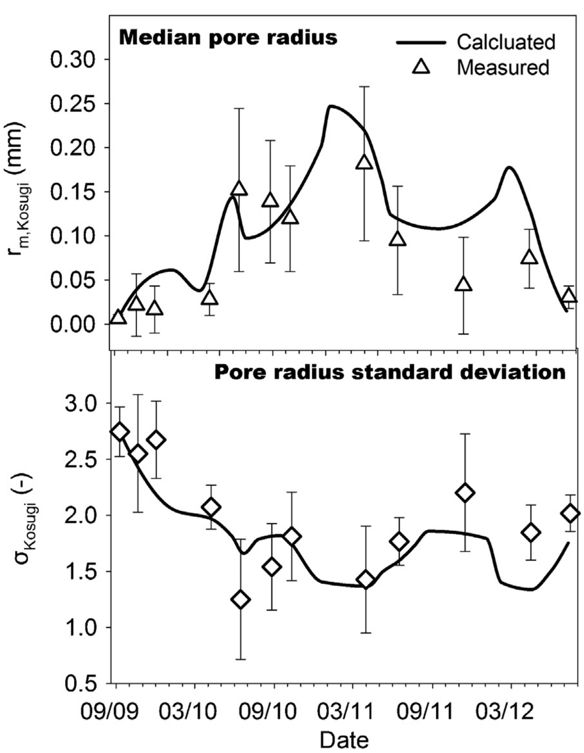

Fig. 8. Time course of soil hydraulic parameters, predicted by the regression models shown in Fig. 7, compared to the range of measured values (means ± SD).

Table 4
Goodness of fit indices for measured and predicted hydraulic property parameters.

	$r_{m,Kosugi}$	σ_{Kosugi}
RMSE	0.035	0.29
EF	0.58	0.60
d	0.89	0.88
r^2 (slope)	0.84 (0.89)	0.86 (0.96)

hydraulic parameters are a better representation of the observed dynamic behavior than using average values. A modeling efficiency (EF) greater 0 indicates that the agreement between the single measured and estimated values is better than using the average of measurement. The values of 0.58 and 0.60 for EF therefore confirm the substantial improvement in capturing the system dynamics when using dynamic parameters predicted by our model. This confirms the conclusion of Schwen et al. (2011) that the reliability of water transport simulation could be improved when using a dynamic instead of a static hydraulic property description.

4. Conclusions

This study presents a quantification of WD cycles from field water content time series using spectral analysis. The method allows extracting the basic characteristics of WD (cycle intensity, number and duration) from the complex and irregular pattern that is typically observed under field conditions. WD cycle intensity was strongly related to the temporal drift in the median pore radius and pore radius standard deviation of Kosugi's water retention model. This confirms laboratory findings that WD cycle intensity is a dominant driving factor of structural porosity which is also valid under field conditions. The effect of cycle intensity was mediated by soil moisture, with dry soil reducing its impact on the hydraulic parameters. Using a bivariate regression model we showed that WD intensity increased macroporosity while decreasing pore heterogeneity. During a general drying phase, expressed in our model by a high cumulative ET_0 or high climatic water balance deficit, the median pore radius was reduced while pore heterogeneity increased due to higher frequency of small pore radius classes. This probably reflects the effect of capillary driven aggregate coalescence. We demonstrated that temporal changes in pore size distribution could be predicted from environmental variables. The modeled values captured the observed system dynamics substantially better than a static representation with averaged parameters. Time series of water content or pressure head are frequently measured in hydrological field studies. Spectral analysis provides a method to make additional use of such measurements by extracting quantitative information on the

WD pattern. Our study confirmed that WD is an important driver of within-season variability of structure related soil properties and processes. Therefore the application of spectral analysis can enhance our understanding of pore and aggregate temporal dynamics under field conditions and provide an important link to laboratory investigations. Further investigations could use this method for quantitatively assessing the interactions of WD with other relevant factors driving temporal changes in the soil pore size distribution such as tillage, irrigation and crop rotation.

Acknowledgement

The present study was funded by the Austrian Science Foundation (FWF) by grant number P 21836-B16. The authors are grateful for the financial support provided to their work.

References

Angulo-Jaramillo, R., Moreno, F., Clothier, B.E., Thony, J.L., Vachaud, G., Fernandez-Boy, E., Cayuela, J.A., 1997. Seasonal variation of hydraulic properties of soils measured using a tension disk infiltrometer. Soil Science Society of America Journal 61, 27–32.

Basma, A.A., Al-Homoud, A.S., Husein Malkawi, A.I., Al-Bashabsheh, M.A., 1996. Swelling–shrinkage behavior of natural expansive clays. Applied Clay Science 11, 211–227.

Baumgartl, T., Horn, R., 1999. Influence of mechanical and hydraulic stresses on hydraulic properties of swelling soils. In: van Genuchten, M.Th., et al. (Eds.),Characterization and Measurement of the Hydraulic Properties of Unsaturated Porous Media. Univ. of Calif., Riverside, pp. 449–457.

Bodner, G., Loiskandl, W., Buchan, G., Kaul, H.-P., 2008. Natural and management-induced dynamics of hydraulic conductivity along a cover-cropped field slope. Geoderma 146, 317–325.

Bodner, G., Scholl, P., Loiskandl, W., Kaul, H.-P., 2013. Environmental and management influences on temporal variability of near saturated soil hydraulic properties. Geoderma 204–205, 120–129.

Braudeau, E., Frangi, J.P., Mohtar, R.H., 2004. Characterizing nonrigid aggregated soil–water medium using its shrinkage curve. Soil Science Society of America Journal 68, 359–370.

Bruand, A., Prost, R., 1987. Effect of water content on the fabric of a soil material: an experimental approach. Journal of Soil Science 38, 461–472.

Cresswell, H.P., Smiles, D.E., Williams, J., 1992. Soil structure, soil hydraulic properties and the soil water balance. Australian Journal of Soil Research 30, 265–283.

Dalal, R.C., Bridge, B.J., 1996. Aggregation and organic matter storage in sub-humid and semi-arid soils. In: Carter, M.R., Stewart, B.A. (Eds.), Structure and Organic Matter Storage in Agricultural Soils. CRC, Boca Raton, FL, pp. 263–308.

Fila, G., Bellocchi, G., Acutis, M., Donatelli, M.M., 2003. IRENE: a software to evaluate model performance. European Journal of Agronomy 18, 369–372.

Hayashi, Y., Kosugi, K., Mizuyama, T., 2006. Changes in pore size distribution and hydraulic properties of forest soil resulting from structural development. Journal of Hydrology 331, 85–102.

Horn, R., Baumgartl, Th., 2002. Dynamic properties of soils. In: Warrick, A.W. (Ed.), Soil Physics Companion. CRC Press, Boca Raton, FL.

Horn, R., Smucker, A., 2005. Structure formation and its consequences for gas and water transport in unsaturated arable and forest soils. Soil and Tillage Research 82, 5–14.

IUSS, 2007. World Reference Base for Soil Resources. FAO, Rome.

Kosugi, K., 1996. Lognormal distribution model for unsaturated soil hydraulic properties. Water Resources Research 32, 2697.

Kutílek, M., Jenele, L., Panayiotopoulos, K.P., 2006. The influence of uniaxial compression upon pore size distribution in bi-model soils. Soil and Tillage Research 86, 27–37.

Lado, M., Paz, A., Ben-Hur, M., 2004. Organic matter and aggregate-size interactions in saturated hydraulic conductivity. Soil Science Society of America Journal 68, 234–242.

Leij, F.J., Ghezzehei, T.A., Or, D., 2002. Modelling the dynamics of the soil pore-size distribution. Soil and Tillage Research 64, 61–78.

Littell, R.C., Henry, P.R., Ammerman, C.B., 1998. Statistical analysis of repeated measures data using SAS procedures. Journal of Animal Science 76, 1216–1231.

Mapa, R.B., Green, R.E., Santo, L., 1986. Temporal variability of soil hydraulic properties with wetting and drying subsequent to tillage. Soil Science Society of America Journal 50, 1133–1138.

Mubarak, I., Mailhol, J.C., Angulo-Jaramillo, R., Ruelle, P., Boivin, P., Khaledian, M., 2009. Temporal variability in soil hydraulic properties under drip irrigation. Geoderma 150, 158–165.

Nielsen, D.R., Wendroth, O., 2003. Spatial and Temporal Statistics Samplin Field Soils and their Vegetation. Catena Publisher, Reiskirchen, Germany.

Oztas, T., Fayetorbay, F., 2003. Effect of freezing and thawing processes on soil aggregate stability. Catena 52, 1–8.

Pagliai, M., La Marca, M., Lucamante, G., 1987. Changes in Soil Porosity in Remolded Soils Treated with Poultry Manure. Soil Science 144, 128–140.

Pagliai, M., Vignozzi, N., Pellegrini, S., 2004. Soil structure and the effect of management practices. Soil and Tillage Research 79, 131–143.

Peng, X., Horn, R., Smucker, A., 2007. Pore shrinkage dependency of inorganic and organic soils on wetting and drying cycles. Soil Science Society of America Journal 71, 1095–1103.

Phogat, V.K., Aylmore, L.A.G., 1989. Evaluation of soil structure by using computer-assisted tomography. Australian Journal of Soil Research 27, 313–323.

Piepho, H.P., Büchse, A., Richter, C., 2004. A mixed modelling approach for randomized experiments with repeated measures. Journal of Agronomy and Crop Science 190, 230–247.

Pires, L.F., Reichardt, K., Cooper, M., Cássarol., F., Dias, N.M.P., Bacchi, O.O.S., 2009. Pore system changes of damaged Brazilian oxisols and nitosols induced by wet-dry cycles as seen in 2-D micromorphologic image analysis. Anais da Academia Brasileira de Ciências 81, 151–161.

Pires., L.F., Bacchi, O.O.S., Reichardt, K., 2005. Gamma ray computed tomography to evaluate wetting/drying soil structure changes. Nuclear Instruments and Methods in Physics Research B 42, 857–863.

Sarmah, A.K., Pillai-McGarry, U., McGarry, D., 1996. Repair of the structure of a compacted Vertisol via wet/dry cycles. Soil and Tillage Research 38, 17–33.

Sartori, G., Ferrari, G.A., Pagliai, M., 1985. Changes in soil porosity and surface shrinkage in a remolded, saline clay soil treated with compost. Soil Science 139, 523–530.

SAS/STAT, 2009. The SPECTRA Procedure. SAS/STAT 9.2 User's Guide, 2nd ed..

Schaap, M.G., Leij, F.J., van Genuchten, M.T., 2001. ROSETTA: a computer program for estimating soil hydraulic parameters with hierarchical pedotransfer functions. Journal of Hydrology 251, 163–176.

Schwen, A., Bodner, G., Scholl, P., Buchan, G.D., Loiskandl, W., 2011. Temporal dynamics of soil hydraulic properties and the water-conducting porosity under different tillage. Soil and Tillage Research 113, 89–98.

Seguel, O., Horn, R., 2006. Structure properties and pore dynamics in aggregate beds due to wetting and drying cycles. Journal of Plant Nutrition and Soil Science 169, 221–232.

Si, B.C., 2008. Spatial scaling analyses of soil physical properties. A review of spectral and wavelet methods. Vadose Zone Journal 7, 547–562.

Šimůnek, J., 2006. PC progress discussion forum. www.pc-progress.com/forum/viewtopic.php?f=3&t=699 (last accessed 15.02.13).

Šimůnek, J., van Genuchten, M.T., 1996. Estimating unsaturated soil hydraulic properties from tension disc infiltrometer data by numerical inversion. Water Resources Research 32, 2683–2696.

Šimůnek, J., van Genuchten, M.T., Sejna, M., 2006. The HYDRUS Software Package for Simulating the Two- and Three-Dimensional Movement of Water, Heat, and Multiple Solutes in Variably-Saturated Media. Technical Manual PC Progress, Prague, Czech Republic.

Šimůnek, J., Angulo-Jaramillo, R., Schaap, M.G., Vandervaere, J.P., van Genuchten, M.T., 1998. Using an inverse method to estimate the hydraulic properties of crusted soils from tension-disc infiltrometer data. Geoderma 86, 61–81.

Torrence, C., Compo, G.T., 1998. A practical guide to wavelet analysis. Bulletin of the American Meteorological Society 79, 61–78.

Tripathy, S., Subba Rao, K.S., Fredl, D.G., 2002. Water content–void ratio swell–shrink paths of compacted expansive soils. Canadian Geotechnical Journal 39, 938–959.

Unger, P.W., 1991. Overwinter changes in physical properties of no-tillage soil. Soil Science Society of America Journal 55, 778–782.

Van Es, H.M., Ogden, C.B., Hill, R.L., Schindelbeck, R.R., Tsegaye, T., 1999. Integrated assessment of space time, and management-related variability of soil hydraulic properties. Soil Science Society of America Journal 63, 1599–1608.

Watts, C.W., Dexter, A.R., Dumitru, E., Arvidsson, J., 1996. An assessment of the vulnerability of soil structure to destabilisation during tillage. Part I. A laboratory test. Soil and Tillage Research 37, 161–174.

Worrall, F., Burt, T.P., 1998. Decomposition of river water nitrate time-series – comparing agricultural and urban signals. Science of the Total Environment 210–211, 153–162.

Zeng, Ch., Wang, Q., Zhang, F., Zhang, Y., 2013. Temporal changes in soil hydraulic conductivity with different soil types and irrigation methods. Geoderma 193–194, 290–299.